



HHS Public Access

Author manuscript

J Invest Dermatol. Author manuscript; available in PMC 2012 August 01.

Published in final edited form as:

J Invest Dermatol. 2012 February ; 132(2): 448–457. doi:10.1038/jid.2011.297.

Fibronectin expression determines skin cell motile behavior

Kevin J. Hamill^{1,2}, Susan B. Hopkinson^{1,2}, Paul Hoover², Viktor Todorovi³, Kathleen J. Green^{2,3}, and Jonathan C.R. Jones^{1,2}

¹Department of Cell and Molecular Biology, Feinberg School of Medicine, Northwestern University, 303 E. Chicago Avenue, Chicago, IL 60611

²Department of Dermatology, Feinberg School of Medicine, Northwestern University, 303 E. Chicago Avenue, Chicago, IL 60611

³Department of Pathology, Feinberg School of Medicine, Northwestern University, 303 E. Chicago Avenue, Chicago, IL 60611

Abstract

Mouse keratinocytes migrate significantly slower than their human counterparts in vitro on uncoated surfaces. We tested the hypothesis that this is a consequence of differences in the extracellular matrix (ECM) that cells deposit. In support of this, human keratinocyte motility was dramatically reduced when plated onto the ECM of mouse skin cells whereas the latter cells migrated faster when plated onto human keratinocyte ECM. The ECM of mouse and human keratinocytes contained similar levels of the $\alpha 3$ laminin subunit of laminin-332. However, mouse skin cells expressed significantly more fibronectin (FN) than human cells. To assess whether FN is a motility regulator, we utilized siRNA to reduce expression of FN in mouse keratinocytes. The treated mouse keratinocytes moved significantly more rapidly than wild-type mouse skin cells. Moreover, the FN depleted mouse cell ECM supported increased migration of both mouse and human keratinocytes. Furthermore, the motility of human keratinocytes was slowed when plated onto FN-coated substrates or human keratinocyte ECM supplemented with FN in a dose dependent manner. Consistent with these findings, the ECM of $\alpha 3$ integrin-null keratinocytes, which also migrated faster than wild-type cells, was FN deficient. Our results provide evidence that FN is a brake to skin cell migration supported by laminin-332-rich matrices.

Introduction

Skin cell migration is an essential aspect of epidermal wound repair and carcinogenesis and is coupled with localized compositional and organizational modification of the ECM as well as changes in expression and activities of a variety of matrix receptors. In the skin, two major ECM proteins, namely laminin $\alpha 3\beta 3\gamma 2$ (LM332, formerly laminin-5;) and FN are

Users may view, print, copy, and download text and data-mine the content in such documents, for the purposes of academic research, subject always to the full Conditions of use:http://www.nature.com/authors/editorial_policies/license.html#terms

Address correspondence to: Jonathan Jones, Department of Cell and Molecular Biology, Feinberg School of Medicine, Northwestern University, 303 E. Chicago Ave, Chicago, IL 60611, Tel. 312 503 1412, FAX. 312 503 6475, j-jones3@northwestern.edu.

Conflicts of interest

None.

upregulated during times of epithelial migration and both have been reported to support cell motility (Aumailley *et al.*, 2005; Clark, 1990; Clark *et al.*, 1982; Natarajan *et al.*, 2006; Nickoloff *et al.*, 1988). However, there are also published data indicating that LM332 and FN inhibit migration of human keratinocytes (Kim *et al.*, 1992; Morla *et al.*, 1994; Natarajan *et al.*, 2006; O'Keefe *et al.*, 1985; O'Toole *et al.*, 1997; Zhang and Kramer, 1996). These conflicting data may reflect functional diversity of the matrix molecules resulting from their post-translational modification. Such is the case with regard to LM332. Unprocessed LM332 functions to support migration while proteolytically cleaved LM332 stabilizes adhesion to substrate by inducing hemidesmosome assembly (Goldfinger *et al.*, 1998). Alternatively, matrix components might either support or impede motility depending on their microenvironment, including availability of cell surface receptors and other binding partners. In this regard, there is extensive evidence that matrix receptors are modulated by cell and tissue context. For example, in keratinocytes, $\alpha 6 \beta 4$ integrin, a receptor for LM332, retards migration when incorporated into hemidesmosomal adhesions but activates pathways that support cell migration in motile cells during tumorigenesis and wound healing (Pullar *et al.*, 2006; Rabinovitz *et al.*, 1999; Sehgal *et al.*, 2006; Shaw *et al.*, 1997; Xia *et al.*, 1996; Zahir *et al.*, 2003). A similar situation may also exist for a second LM332 receptor, namely $\alpha 3 \beta 1$ integrin, since there are reports that it functions as both a positive and negative regulator of keratinocyte migration (Hodivala-Dilke *et al.*, 1998; Margadant *et al.*, 2009; Reynolds *et al.*, 2008; Wen *et al.*, 2010).

Many advances in our understanding of how ECM components and their receptors regulate skin cell motility have been made in vitro using primary and immortalized keratinocytes derived from normal and genetically modified mice as well as normal and diseased human skin (Hodivala-Dilke *et al.*, 1998; Margadant *et al.*, 2009; Marinkovich *et al.*, 1992; Nguyen *et al.*, 2000a; Nickoloff *et al.*, 1988; O'Keefe *et al.*, 1985; O'Toole *et al.*, 1997; Pullar *et al.*, 2006; Sehgal *et al.*, 2006). The considerable recent improvements in the culture media of both mouse and human keratinocytes prompted us to undertake a comparison of the motility of primary and immortalized mouse and human skin cells in some of these new media formulations. Surprisingly, our results indicate that mouse keratinocytes move much slower than their human counterparts when maintained in commonly used, serum-free, media. We investigated the reason for this disparity and provide data indicating that the motility of mouse keratinocytes is impeded by their deposition of FN into their matrix, a finding at odds with previous results (Kim *et al.*, 1992; Nickoloff *et al.*, 1988; O'Keefe *et al.*, 1985). As part of our analyses we also demonstrate that $\alpha 3$ integrin-null cells are deficient in FN deposition and discuss this result in relation to the conflicting reports concerning $\alpha 3 \beta 1$ integrin and its role in keratinocyte motility.

Results and Discussion

We first analyzed the migration of passage 2 human foreskin and passage 2 C57/B16 newborn mouse keratinocytes (pHEK and pMEK, respectively) along with immortalized human and mouse keratinocyte lines (iHEK and iMEK, respectively). For the current studies, all of our cells were maintained in serum-free conditions and in low (0.07mM) calcium medium. We chose passage 2 primary mouse cells for this study because primary murine keratinocytes were difficult to maintain in culture after more than 3 passages. Our

migration assays involved plating keratinocytes overnight onto uncoated glass bottomed dishes and then imaging cells every 2 mins over 1 hour. Migration paths of individual cells were tracked using Metamorph software and mean migration rates calculated (Fig 1a,b). These assays and time course were selected as they allow sufficient time for cells to deposit and organize their own ECM prior to the start of the study. Interestingly, pMEK migrated significantly slower than their human counterparts while the migration rates of pHEKs were significantly slower than iHEKs (total displacement rates: pMEK 0.68 ± 0.09 $\mu\text{m}/\text{min}$, iMEK 0.57 ± 0.01 $\mu\text{m}/\text{min}$, pHEK, 0.95 ± 0.07 $\mu\text{m}/\text{min}$, iHEK 1.35 ± 0.08 $\mu\text{m}/\text{min}$). There was no significant difference in processivity (the ratio of net displacement to total displacement) between pMEKs and pHEKs or between iMEKs and iHEKs (Supplemental Fig 1a). Intriguingly, however, both primary lines displayed more intrinsic processivity compared to their immortalized counterparts (0.52 ± 0.14 to 0.37 ± 0.04 pMEK to iMEK, 0.50 ± 0.09 to 0.31 ± 0.06 pHEK to iHEK) (Supplemental Fig 1a).

Next, we sought to determine whether the slower migration rates of the MEK lines was due to inherent differences in the cytoplasmic motile machinery of mouse versus human keratinocytes or due to differences in the ECM these cells deposit. As a first test of this we plated iHEKs and iMEKs at near confluence overnight onto glass bottomed dishes and then used ammonium hydroxide treatment to remove cellular material, leaving ECM material behind (Gospodarowicz *et al.*, 1980). We have previously shown that this technique yields a substrate enriched in ECM material and capable of supporting both cell attachment and migration (Langhofer *et al.*, 1993a; Sehgal *et al.*, 2006; Todorovic *et al.*, 2010a). iHEKs or iMEKs were plated onto these prepared matrices, allowed to adhere and spread for 2 hours, and then their motile behavior was analyzed. This shorter pre-assay attachment period was selected to minimize the contribution of ECM deposition by the freshly plated cells on their own motility. As expected iMEKs on iMEK ECM and iHEKs on iHEK ECM displayed motility rates that were not significantly different from those when the same cells were plated overnight onto uncoated glass (Fig 1c,d). However, iHEKs plated on iMEK ECM migrated markedly slower than iHEKs on iHEK ECM (0.88 ± 0.25 $\mu\text{m}/\text{min}$ versus 1.33 ± 0.29 $\mu\text{m}/\text{min}$, Fig 1c). Conversely, iMEKs plated onto iHEK ECM exhibit a modest but significant increase in their motility rates relative to iMEKs on iMEK ECM (0.76 ± 0.01 $\mu\text{m}/\text{min}$ versus 0.64 ± 0.03 $\mu\text{m}/\text{min}$, Fig 1c). There were no clear differences in processivity of human and mouse cells regardless of matrix used in these studies (Supplemental Fig 1b). Nevertheless, these data suggest that the ECM deposited by iMEKs is an inferior substrate for keratinocyte migration than the ECM of iHEKs.

To assess the possibility that these difference were related to the ECM molecules that the cells deposit, we undertook immunoblotting of cell lysates and ECM extracts of iMEKs and iHEKs for two major keratinocyte ECM constituents, $\alpha 3$ laminin and FN, (Aumailley *et al.*, 2005; Clark, 1990; Clark *et al.*, 1982; Nickoloff *et al.*, 1988). The matrices of iMEKs and iHEKs contained FN and $\alpha 3$ laminin (Fig. 2a). However, there was more FN in the iMEK versus iHEK ECM. Immunofluorescence analyses using FN and LM 332 antibodies supported these observations (Fig 2b,c). FACS analyses revealed that the relative deficiency of FN in HEK matrix was not the result of a lack of surface expression of the FN receptor $\alpha 5 \beta 1$ integrin by iHEKs (Fig 2d).

To assess whether the above findings were applicable to other keratinocyte cell lines, we also assessed the motility and FN expression of two additional immortalized human (HaCaT, SCC25) and one immortalized mouse (PAM) skin cell lines, all of which are maintained in serum-containing media (Boukamp *et al.*, 1988; Hu *et al.*, 1991; Jones *et al.*, 1982). All three lines expressed FN at levels which greatly exceeded that of iHEKs (Supplemental Fig 2a). They all stained positively for both FN and LM332 with the latter being restricted within cell boundaries (Supplemental Fig 2e, f). This pattern was quite distinct from that observed in iHEKs where LM332 antibody staining reveals extensive tracks outside cell borders (Fig 2d). In addition to this difference, the migration rates of the HaCaT, SCC25 and PAM cells were significantly slower than iHEKs (HaCaT 0.67 ± 0.05 , SCC25 0.60 ± 0.03 , PAM212 0.66 ± 0.05 $\mu\text{m}/\text{min}$; Supplemental Fig 2b,c and d).

Our analyses of the matrices deposited by MEK and HEK raised the possibility that the differences in keratinocyte migration rates supported by iMEK and iHEK ECMs was related to either differential proteolytic processing of $\alpha 3$ laminin or to the level of FN within each matrix. The former possibility seemed unlikely since it has been reported that matrices enriched in the unprocessed form of $\alpha 3$ laminin supported migration while matrices enriched in the processed form supported stable adhesion of keratinocytes (Goldfinger *et al.*, 1998). iMEK ECM contained more 190kD unprocessed than 160kD processed $\alpha 3$ laminin and, hence, might be expected to support more rapid cell motility (Goldfinger *et al.*, 1998). Although this result does not rule out that the differences in motility rates reflect differential processing of the $\gamma 2$ or $\beta 3$ subunits, we tested an alternative hypothesis that FN in the matrix of the mouse keratinocytes was the contributing factor to the lower migration rates that iMEK matrix supported (Natarajan *et al.*, 2006; Udayakumar *et al.*, 2003). To do so, we utilized transient transfection of siRNA against the FN message to reduce FN expression in iMEKs (Fig 3a). Transfected cells were plated onto glass bottomed dishes and motility behavior analyzed. FN knockdown iMEKs exhibited significantly faster motility than control siRNA treated cells (0.86 ± 0.14 $\mu\text{m}/\text{min}$ versus 0.57 ± 0.1 $\mu\text{m}/\text{min}$, Fig 3b,c). We also plated iMEKs and iHEKs onto the ECM derived from FN-deficient iMEKs and assessed their motility relative to iMEKs plated on control iMEK ECM (Fig 3b). Results indicated that the matrix elaborated by FN-deficient iMEKs supported more rapid migration than the ECM of iMEKs for both iMEKs and iHEKs (Fig 3b, iMEKs 0.79 ± 0.15 $\mu\text{m}/\text{min}$ on FNsiRNA ECM versus 0.64 ± 0.07 $\mu\text{m}/\text{min}$ on iMEK ECM, iHEKs 1.21 ± 0.25 on FNsiRNA ECM versus 0.83 ± 0.18 $\mu\text{m}/\text{min}$ on iMEK ECM). Moreover iMEK and iHEK migration rates on the FN-knockdown ECM mirrored their motility rate when they were plated onto the ECM derived from iHEKs (iMEKs 0.79 ± 0.15 $\mu\text{m}/\text{min}$ on FNsiRNA ECM versus 0.76 ± 0.01 $\mu\text{m}/\text{min}$ on iHEK ECM, iHEK 1.21 ± 0.25 $\mu\text{m}/\text{min}$ on FNsiRNA ECM versus 1.33 ± 0.29 $\mu\text{m}/\text{min}$ on iHEK ECM). No significant differences in processivity was observed for mouse skin cells exhibiting FN knockdown or for keratinocytes plated onto the fibronectin-depleted matrix deposited by mouse keratinocytes (Supplemental Fig 1c). These results were consistent with a recent report in which plakoglobin-null MEKs were shown to display 50 fold decreased FN expression compared to expression of plakoglobin-expressing mouse skin cells and to exhibit increased migration rates (Todorovic *et al.*, 2010b).

To determine if cell-mediated deposition and/or organization of FN was required for its inhibitory effect or whether its presence was sufficient to slow migration, we analyzed the motile behavior of iHEKs and FN siRNA treated iMEKs plated onto dishes coated with soluble FN (Fig 3d,e, Supplemental Fig 1d). For both populations, significant reductions in motility rates were observed when plated on FN versus their own matrix. We next sought to determine if addition of soluble FN to iHEK-derived, laminin-332 rich-matrix influenced the migration rate of iHEKs plated upon it. iHEKs plated onto iHEK ECM supplemented with FN migrated significantly slower than those plated onto iHEK ECM lacking any supplement (Fig 3f,g, Supplemental Fig 1e). Moreover, the migration rate of HEKs on HEK matrix decreased with increasing FN concentration (0.01 μ g/ml FN; 1.02 \pm 0.05, 0.1 μ g/ml FN; 1.00 \pm 0.09, 1 μ g/ml 0.88 \pm 0.07, 10 μ g/ml; 0.65 \pm 0.06 μ m/min).

Cell migration rates have been demonstrated to possess a biphasic relationship with adhesive strength, with intermediate ECM coating concentrations providing optimal conditions for rapid migration (DiMilla *et al.*, 1993; Macdonald *et al.*, 2008; Palecek *et al.*, 1997). These published observations suggested the possibility that FN inhibited migration of keratinocytes migrating on LM332 due to its ability to enhance cell adhesion. To test this, we evaluated attachment of iHEKs to uncoated surfaces or surfaces coated with LM332-rich conditioned medium, with and without FN. iHEKs attach more readily to FN coated surfaces even in the presence of LM332, suggesting that in our studies FN inhibited migration, at least in part, by enhancing cell adhesion to substrate (Fig 3h).

Intriguingly, our initial analyses of passage 2 human primary keratinocytes revealed that although they migrated significantly more rapidly than the equivalent passage of primary mouse keratinocytes, their mean migration rate was significantly slower than the iHEKs (Fig 1a). Previously, it was demonstrated that FN expression decreased in fibroblastic cells with increasing passages and transformation (Yamada *et al.*, 1977). Increased passage number in human keratinocytes has also been demonstrated to correspond to increased migration rates (Sutherland *et al.*, 2005). We therefore assessed the FN expression and motility rates of human primary keratinocytes with increasing passage number (p2–p3, 11–16 days post isolation, Fig 4a, b and c). Results indicate that FN expression decreased dramatically with increasing passage and that this decrease correlated with an increase in migration rate (Fig 4a and b, p2 0.58 \pm 0.03 μ m/min versus p3 0.81 μ m/min). Moreover, although the processivity of primary keratinocytes was higher than the immortalized line, processivity decreased with increasing passage number (supplemental Fig 1f, iHEK 0.3 \pm 0.06, pHEK p2 0.5 \pm 0.09, pHEK p3 0.42 \pm 0.11).

We wondered whether differential expression of FN might explain contradictory findings regarding the function of a major keratinocyte ECM receptor α 3 β 1 integrin in migration. In brief, antibody blockade of α 3 β 1 integrin inhibits migration of human keratinocytes on a LM332 substrate whereas mouse keratinocytes deficient in α 3 integrin (iMEK α 3-) exhibit enhanced migration (Fig 5a,b; iMEKs 0.57 \pm 0.01 μ m/min versus iMEK α 31 0.73 \pm 0.09 μ m/min). (deHart *et al.*, 2003; Frank and Carter, 2004; Giannelli *et al.*, 1997; Goldfinger *et al.*, 1999; Margadant *et al.*, 2009; Reynolds *et al.*, 2008) Remarkably, we detected no FN in extracts of iMEK α 3- cells or their matrix (Fig. 5c). Moreover immunofluorescence analyses revealed a lack of FN staining in iMEK α 3- compared whereas LM332 was deposited in

extensive tracks (Fig 5d). The former result was not due to a cell surface change in expression of the FN binding integrin $\alpha 5\beta 1$ since FACS analyses revealed that the cell surface expression levels of $\alpha 5\beta 1$ integrin were similar in MEKs and iMEK $\alpha 3$ - (Fig 5e). Moreover, the motility of iMEK $\alpha 3$ - cells was inhibited on FN-coated surfaces, indicating that their enhanced motility in vitro was likely due to their inability to deposit FN into their matrix (Fig 5a,b, iMEK $\alpha 3$ - on glass 0.73 ± 0.09 $\mu\text{m}/\text{min}$ versus iMEK $\alpha 3$ - on FN 0.51 ± 0.02 $\mu\text{m}/\text{min}$).

The data we present here raise some new questions about the differences between cultured mouse and human keratinocytes, the matrix they deposit and the mechanisms of their motility. Can one directly compare motility data from cultured mouse and human keratinocytes or even mouse cells of different genetic backgrounds? Our results argue that to do so one must first perform analyses of the matrix they deposit. In the absence of FN, what are the iMEK $\alpha 3$ - cells migrating upon? Based upon our prior analyses of human keratinocyte migration we suggest that their motility is supported on the LM332 they deposit (Goldfinger *et al.*, 1999). Why is FN deposition inhibited in pHEK and iHEK cells in culture compared to pMEK and iMEKs? One possible explanation is that there are differences in the way FN expression is regulated at the transcriptional or translational levels in cultured human versus mouse keratinocytes (Todorovic *et al.*, 2010b). Alternatively, the apparent loss of FN levels in the matrix of human skin cells may be due to differences in activation and/or expression of cell surface receptors involved in matrix protein expression, deposition and assembly. This would be consistent with the data we present regarding FN deposition by iMEK $\alpha 3$ - cells. Do our results have relevance to skin wound repair in vivo? In a deep wound, in which the basement membrane zone is compromised, keratinocytes migrate over a provisional fibrinogen/FN matrix covering the wound bed (Clark, 1990; Clark *et al.*, 1982). It has long been assumed that this FN-rich matrix supports migration of keratinocytes (Nickoloff *et al.*, 1988; O'Keefe *et al.*, 1985). Our results argue that, in this context, enhanced wound healing would be observed in areas where keratinocytes are exposed to a matrix containing a reduced rather than an increased FN content. In the wound environment motile keratinocytes deposit a matrix enriched in unprocessed LM332, demonstrated to support motility (Larjava *et al.*, 1993; Marinkovich *et al.*, 1992; Nguyen *et al.*, 2000b; Zhang and Kramer, 1996). Thus, it is tempting to speculate that keratinocyte motility during skin repair is, in part, regulated by the balance between the negative and positive effects of FN and LM332 present along the wound bed. Analyses of wound healing in vivo will be required to test such a possibility.

Materials and Methods

Antibodies

Rabbit polyclonal antibodies against FN and $\alpha 5\beta 1$ integrin were purchased from Sigma Aldrich (St Louis, MO) and Abcam (Cambridge MA), respectively. Antibodies against lamin, a component of the nuclear lamina, were obtained from Cell Signaling Technology (Beverly, MA). Monoclonal antibody 10B5 against the $\alpha 3$ laminin subunit and rabbit serum J18 against all three subunits of LM332 were described previously (Goldfinger *et al.*, 1998;

Langhofer *et al.*, 1993b). Mouse monoclonal antibodies against human $\alpha 5\beta 1$ integrin (mAb 1969) and $\alpha 3$ (mAb 2056) were obtained from Millipore (Billerica, MA).

Secondary antibodies conjugated with various fluorochromes or horseradish peroxidase were purchased from Jackson ImmunoResearch Laboratories Inc. (West Grove, PA).

Tissue Culture

Mice were maintained in accordance with local governmental and institutional animal care regulations and all procedures had institutional approval (Northwestern University IACUC protocol number 2008-0215) Mouse keratinocytes were isolated from newborn C57/B16 wild-type and, $\alpha 3$ integrin-null mice (deHart *et al.*, 2003). Briefly, the skin of less than 1 day old pups was incubated in 5 mg/ml dispase solution (Sigma) overnight at 4°C. Following incubation, the dermal and epidermal layers were separated using 2 pairs curved forceps and the epidermis transferred and spread onto a 500 μ l drop of TrypLE Select (Invitrogen). Following 30 mins incubation at room temperature, epidermal cells were dissociated by scraping, then pelleted (160g, 5 min) and plated at 5×10^4 cells/cm² in Cnt07 complete media (CELLnTEC, Bern, Switzerland). Keratinocytes isolated as above were immortalized through infection with SV40 large T antigen (MOI 0.5) with media replaced every 3–4 days until keratinocytes cleared senescence (Steinberg and Defendi, 1979),

Human primary keratinocytes were isolated from de-identified human foreskins obtained from routine circumcisions performed on neonates at Prentice women's hospital, Chicago, IL (IRB project #STU00002257). Foreskins were washed extensively with PBS, cut into small pieces and incubated overnight on dispase (Sigma) at 4°C. The following day, the dermis and epidermis were separated using sterile forceps and the epidermis incubated at 37°C for 10 minutes in 0.25% trypsin/1mM EDTA solution. Following digestion, cells were dissociated from the tissue through scraping, filtered through a 40 μ m sieve. Cells were pelleted (220 \times g 5min) and resuspended in M154 keratinocyte growth media (Epilife, Cascade biologics, Portland, OR), supplemented with 0.07mM CaCl₂, human keratinocyte growth supplement that includes 0.18% hydrocortisone, 5 μ g/ml transferrin, 0.2% vol/vol bovine pituitary extract, 0.2 ng/ml EGF, and 5 μ g/ml insulin), gentamicin (10 μ g/ml) amphotericin B (0.25 μ g/ml)(Cascade biologics). Human keratinocytes isolated as above, were immortalized in the lab of Dr Lou Laimins at Northwestern University using human papilloma virus *E6* and *E7* genes (Kaur *et al.*, 1989). Immortalized HEKs were maintained in defined keratinocyte serum-free medium (DKSFM)(0.07mM CaCl₂), supplemented with a proprietary growth factor mixture (serum and bovine pituitary extract free)(Invitrogen). HaCaT, 3T3 fibroblasts and PAM lines were maintained in Dulbecco's modified Eagle Medium (DMEM, Invitrogen) supplemented with 10% Fetal Bovine Serum (FBS, Hyclone, Logan UT). SCC25 were maintained in DMEM/F12 mixture (Invitrogen) supplemented with FBS. All cell lines were maintained at 37°C in a 5% CO₂ humidified environment.

For FN coatings, glass bottomed dishes were incubated with soluble FN (Sigma Aldrich, 50 μ g/ml) in PBS for 1 hour. For siRNA experiments, iMEKs were plated overnight at 1×10^5 cells/well in 6 well dishes. 24 later cells were transfected to a final concentration of 100nM with either siRNA targeting FN (5' AACAAATCTCCTGCCTGGGAC 3', Qiagen, Chatsworth, CA) or a validated scrambled control siRNA (Qiagen) using Fugene 6

transfection reagent (Roche Applied Bioscience, Indianapolis, IN) following manufacturer's recommendations. 48h following transfection, cells were trypsinized, pooled and replated for analysis.

Extracellular matrix preparations

Cell derived extracellular matrix preparations were prepared as described previously, (Langhofer *et al.*, 1993). Briefly, cells were plated and allowed to reach 80–90% confluency on tissue culture dishes or glass bottomed dishes. The culture medium was removed and the cells were washed in sterile phosphate-buffered saline (PBS). Cells were ruptured and cellular material removed by treating them with sterile 20 mM NH₄OH (Sigma Aldrich) for 5 min, followed by three rapid washes in sterile PBS. Keratinocytes were either plated directly onto the prepared substrates or following 1 hour of incubation with either PBS or 0.01 – 10 µg/ml FN in PBS as indicated.

Cell Motility Assays

Single cell motility was measured as detailed by us previously (Sehgal *et al.*, 2006). Briefly, cells were plated onto 35-mm glass-bottomed culture dishes (MatTek Corp., Ashland, MA) and allowed to adhere overnight onto uncoated dishes or for 2 hours onto dishes coated with FN or cell derived ECMs. The cells were then viewed on a Nikon TE2000 inverted microscope (Nikon Inc., Melville, NY). Images were taken at 2 min intervals over 1 hour, and cell motility behavior was analyzed using a MetaMorph Imaging System (Universal Imaging Corp., Molecular Devices, Downingtown, PA). Statistical analyses and significance were determined using GraphPad prism software (GraphPad Software, San Diego, CA).

Cell Attachment Assay

Individual wells of a 96-well plate (Sarstedt, Newton, NC) were coated with 10 µg/ml FN in PBS (1h at 37°C), LM332 conditioned media (2h at 37°C), or LM332 conditioned media followed by 10 µg/ml FN. Wells were then blocked in 5% BSA for 1h prior to plating of 1×10^5 iHEKs per well. After 30 or 60 min at 37°C, the cells were washed extensively with PBS to remove non-attached cells. Adherent cells were then fixed in 3.7% formaldehyde in PBS for 15 min at room temperature. The fixed cells were incubated at room temperature with 0.5% crystal violet for 15 min and then solubilized with 1% SDS. A₅₇₀ was measured with a V_{max} plate reader (Molecular Devices, Menlo Park, CA).

Immunofluorescence microscopy, SDS-PAGE and western immunoblotting

Cultured cells on glass coverslips were processed as detailed previously (Sehgal *et al.*, 2006). All preparations were viewed with a confocal laser-scanning microscope (UV LSM 510, Zeiss Inc., Thornwood, NY). Images were exported as TIFF files, and figures were prepared using Adobe Photoshop and Illustrator software.

Total cell lysates and matrix extracts of cells 2 days after plating were prepared as described previously using a sample buffer comprising 8M Urea, 1% SDS, 10mM TrisHCl, pH 6.8 (Langhofer *et al.*, 1993a; Riddelle *et al.*, 1991). Protein samples were processed for SDS-PAGE and immunoblotting as detailed elsewhere (Harlow and Lane, 1988; Riddelle *et al.*, 1991). To control for loading, whole cell lysates and ECMs were prepared from replica

plates seeded with identical numbers of cells (1.5×10^6 cells/100mm dish). Lamin reactivity on western blots was used to confirm equal loading of whole cell lysates. To control for loading of the ECMs, isolated matrix was solubilized in a half the volume of sample buffer used to solubilize whole cell lysates. Equal volumes of cell lysates and ECMs were loaded onto each gel.

Fluorescence-activated Cell Sorting (FACS)

For flow cytometry, freshly trypsinized cells were resuspended in PBS containing a 50% dilution of normal goat serum, incubated with monoclonal antibodies against $\alpha 5\beta 1$ integrin or $\alpha 3\beta 1$ integrin for 45 min at room temperature, washed with PBS, incubated with FITC-conjugated goat anti- mouse IgG for 45 min, washed, resuspended in PBS, and analyzed using a Beckman Coulter Elite PCS sorter (Beckman Coulter, Fullerton, CA). For negative controls, primary antibody was omitted from the above procedure.

Supplementary Material

Refer to Web version on PubMed Central for supplementary material.

Acknowledgements

We would like to thank Lou Laimins of Northwestern University for providing immortalized human keratinocytes. A Dermatology Foundation Research Grant and a Career Development Award supports KH. Work in the Jones laboratory is funded by NIAMS (RO1 AR054184). This research was supported in part by resources provided by the Northwestern University Skin Disease Research Center (5P30AR057216-02), Chicago, IL with support from the NIH/NIAMS. Any opinions, findings, and conclusions or recommendations expressed in this material are those of the authors and do not necessarily reflect the views of the Northwestern University Skin Disease Research Center or the NIH/NIAMS. Imaging work was performed at the Northwestern University Cell Imaging Facility generously supported by NCI CCSG P30 CA060553 awarded to the Robert H Lurie Comprehensive Cancer Center. FACS analyses were performed at the Northwestern University Flow Cytometry Facility supported by a Cancer Center Support Grant (NCI CA060553).

References

- Aumailley M, Bruckner-Tuderman L, Carter WG, Deutzmann R, Edgar D, Ekblom P, et al. A simplified laminin nomenclature. *Matrix Biol.* 2005; 24:326–332. [PubMed: 15979864]
- Boukamp P, Petrussevska RT, Breitkreutz D, Hornung J, Markham A, Fusenig NE. Normal keratinization in a spontaneously immortalized aneuploid human keratinocyte cell line. *J Cell Biol.* 1988; 106:761–771. [PubMed: 2450098]
- Clark RA. Fibronectin matrix deposition and fibronectin receptor expression in healing and normal skin. *J Invest Dermatol.* 1990; 94:128S–134S. [PubMed: 2161886]
- Clark RA, Lanigan JM, DellaPelle P, Manseau E, Dvorak HF, Colvin RB. Fibronectin and fibrin provide a provisional matrix for epidermal cell migration during wound reepithelialization. *J Invest Dermatol.* 1982; 79:264–269. [PubMed: 6752288]
- deHart GW, Healy KE, Jones JCR. The role of $\alpha 3\beta 1$ integrin in determining the supramolecular organization of laminin-5 in the extracellular matrix of keratinocytes. *Exp Cell Res.* 2003; 283:67–79. [PubMed: 12565820]
- DiMilla PA, Stone JA, Quinn JA, Albelda SM, Lauffenburger DA. Maximal migration of human smooth muscle cells on fibronectin and type IV collagen occurs at an intermediate attachment strength. *J Cell Biol.* 1993; 122:729–737. [PubMed: 8335696]
- Frank DE, Carter WG. Laminin 5 deposition regulates keratinocyte polarization and persistent migration. *J Cell Sci.* 2004; 117:1351–1363. [PubMed: 14996912]

- Giannelli G, Falk-Marzillier J, Schiraldi O, Stetler-Stevenson WG, Quaranta V. Induction of cell migration by matrix metalloprotease-2 cleavage of laminin-5. *Science*. 1997; 277:255–228.
- Goldfinger LE, Hopkinson SB, deHart GW, Collawn S, Couchman JR, Jones JC. The alpha3 laminin subunit, alpha6beta4 and alpha3beta1 integrin coordinately regulate wound healing in cultured epithelial cells and in the skin. *J Cell Sci*. 1999; 112(Pt 16):2615–2629. [PubMed: 10413670]
- Goldfinger LE, Stack MS, Jones JCR. Processing of laminin-5 and its functional consequences: role of plasmin and tissue-type plasminogen activator. *J Cell Biol*. 1998; 141:255–265. [PubMed: 9531563]
- Gospodarowicz D, Delgado D, Vlodavsky I. Permissive effect of the extracellular matrix on cell proliferation in vitro. *Proc Natl Acad Sci U S A*. 1980; 77:4094–4098. [PubMed: 6933458]
- Harlow, E.; Lane, D. *Antibodies: A Laboratory Manual*. CSHL Press; 1988. p. 726
- Hodivala-Dilke KM, DiPersio CM, Kreidberg JA, Hynes RO. Novel roles for alpha3beta1 integrin as a regulator of cytoskeletal assembly and as a trans-dominant inhibitor of integrin receptor function in mouse keratinocytes. *J Cell Biol*. 1998; 142:1357–1369. [PubMed: 9732295]
- Hu L, Crowe DL, Rheinwald JG, Chambon P, Gudas LJ. Abnormal expression of retinoic acid receptors and keratin 19 by human oral and epidermal squamous cell carcinoma cell lines. *Cancer Res*. 1991; 51:3972–3981. [PubMed: 1713123]
- Jones JC, Goldman AE, Steinert PM, Yuspa S, Goldman RD. Dynamic aspects of the supramolecular organization of intermediate filament networks in cultured epidermal cells. *Cell Motil*. 1982; 2:197–213. [PubMed: 6756644]
- Kaur P, McDougall JK, Cone R. immortalization of primary human epithelial cells by cloned cervical carcinoma DNA containing human papillomavirus type 16 E6/E7 open reading frames. *J Gen Virol*. 1989; 70(Pt 5):1261–1266. [PubMed: 2543780]
- Kim JP, Zhang K, Chen JD, Wynn KC, Kramer RH, Woodley DT. Mechanism of human keratinocyte migration on fibronectin: unique roles of RGD site and integrins. *J Cell Physiol*. 1992; 151:443–450. [PubMed: 1295896]
- Langhofer M, Hopkinson SB, Jones JC. The matrix secreted by 804G cells contains laminin-related components that participate in hemidesmosome assembly in vitro. *J Cell Sci*. 1993a; 105(Pt 3): 753–764. [PubMed: 8408302]
- Langhofer M, Hopkinson SB, Jones JCR. The matrix secreted by 804G cells contains laminin-related components that participate in hemidesmosome assembly in vitro. *J Cell Sci*. 1993b; 105:753–764. [PubMed: 8408302]
- Larjava H, Salo T, Haapasalmi K, Kramer RH, Heino J. Expression of integrins and basement membrane components by wound keratinocytes. *J Clin Invest*. 1993; 92:1425–1435. [PubMed: 8376596]
- Macdonald A, Horwitz AR, Lauffenburger DA. Kinetic model for lamellipodal actin-integrin 'clutch' dynamics. *Cell Adh Migr*. 2008; 2:95–105. [PubMed: 19262096]
- Margadant C, Raymond K, Kreft M, Sachs N, Janssen H, Sonnenberg A. Integrin $\alpha3\beta1$ inhibits directional migration and wound re-epithelialization in the skin. *J Cell Sci*. 2009; 122:278–288. [PubMed: 19118220]
- Marinkovich MP, Lunstrum GP, Burgeson RE. The anchoring filament protein kalinin is synthesized and secreted as a high molecular weight precursor. *J Biol Chem*. 1992; 267:17900–17906. [PubMed: 1517226]
- Morla A, Zhang Z, Ruoslahti E. Superfibronectin is a functionally distinct form of fibronectin. *Nature*. 1994; 367:193–196. [PubMed: 8114919]
- Natarajan E, Omobono JD 2nd, Guo Z, Hopkinson S, Lazar AJ, Brenn T, et al. A keratinocyte hypermotility/growth-arrest response involving laminin 5 and p16INK4A activated in wound healing and senescence. *Am J Pathol*. 2006; 168:1821–1837. [PubMed: 16723698]
- Nguyen BP, Gil SG, Carter WG. Deposition of laminin 5 by keratinocytes regulates integrin adhesion and signaling. *J Biol Chem*. 2000a; 275:31896–31907. [PubMed: 10926936]
- Nguyen BP, Ryan MC, Gil SG, Carter WG. Deposition of laminin 5 in epidermal wounds regulates integrin signaling and adhesion. *Curr Opin Cell Biol*. 2000b; 12:554–562. [PubMed: 10978889]

- Nickoloff BJ, Mitra RS, Riser BL, Dixit VM, Varani J. Modulation of keratinocyte motility. Correlation with production of extracellular matrix molecules in response to growth promoting and antiproliferative factors. *Am J Pathol.* 1988; 132:543–551. [PubMed: 2458044]
- O’Keefe EJ, Payne RE Jr, Russell N, Woodley DT. Spreading and enhanced motility of human keratinocytes on fibronectin. *J Invest Dermatol.* 1985; 85:125–130. [PubMed: 3894525]
- O’Toole EA, Marinkovich MP, Hoeffler WK, Furthmayr H, Woodley DT. Laminin-5 inhibits human keratinocyte migration. *Exp Cell Res.* 1997; 233:330–339. [PubMed: 9194495]
- Palecek SP, Loftus JC, Ginsberg MH, Lauffenburger DA, Horwitz AF. Integrin-ligand binding properties govern cell migration speed through cell-substratum adhesiveness. *Nature.* 1997; 385:537–540. [PubMed: 9020360]
- Pullar CE, Baier BS, Kariya Y, Russell AJ, Horst BA, Marinkovich MP, et al. beta4 integrin and epidermal growth factor coordinately regulate electric field-mediated directional migration via Rac1. *Mol Biol Cell.* 2006; 17:4925–4935. [PubMed: 16914518]
- Rabinovitz I, Toker A, Mercurio AM. Protein kinase C-dependent mobilization of the alpha6beta4 integrin from hemidesmosomes and its association with actin-rich cell protrusions drive the chemotactic migration of carcinoma cells. *J Cell Biol.* 1999; 146:1147–1160. [PubMed: 10477766]
- Reynolds LE, Conti FJ, Silva R, Robinson SD, Iyer V, Rudling R, et al. alpha3beta1 integrin-controlled Smad7 regulates reepithelialization during wound healing in mice. *J Clin Invest.* 2008; 118:965–974. [PubMed: 18246199]
- Riddelle KS, Green KJ, Jones JC. Formation of hemidesmosomes in vitro by a transformed rat bladder cell line. *J Cell Biol.* 1991; 112:159–168. [PubMed: 1986003]
- Sehgal BU, Debiase P, Matzno S, Chew T-L, Claiborne JN, Hopkinson SB, et al. Integrin beta4 regulates migratory behavior of keratinocytes by determining laminin-332 (laminin-5) matrix organization. *J Biol Chem.* 2006; 281:35487–35498. [PubMed: 16973601]
- Shaw LM, Rabinovitz I, Wang HH, Toker A, Mercurio AM. Activation of phosphoinositide 3-OH kinase by the alpha6beta4 integrin promotes carcinoma invasion. *Cell.* 1997; 91:949–960. [PubMed: 9428518]
- Steinberg ML, Defendi V. Altered pattern of growth and differentiation in human keratinocytes infected by simian virus 40. *Proc Natl Acad Sci U S A.* 1979; 76:801–805. [PubMed: 218222]
- Sutherland J, Denyer M, Britland S. Motogenic substrata and chemokinetic growth factors for human skin cells. *J Anat.* 2005; 207:67–78. [PubMed: 16011545]
- Todorovic V, Desai BV, Eigenheer RA, Yin T, Amargo EV, Mrksich M, et al. Detection of differentially expressed basal cell proteins by mass spectrometry. *Mol Cell Proteomics.* 2010a; 9:351–361. [PubMed: 19955077]
- Todorovic V, Desai BV, Patterson MJ, Amargo EV, Dubash AD, Yin T, et al. Plakoglobin regulates cell motility through Rho- and fibronectin-dependent Src signaling. *J Cell Sci.* 2010b; 123:3576–3586. [PubMed: 20876660]
- Udayakumar TS, Chen ML, Bair EL, Von Bredow DC, Cress AE, Nagle RB, et al. Membrane type-1-matrix metalloproteinase expressed by prostate carcinoma cells cleaves human laminin-5 beta3 chain and induces cell migration. *Cancer Res.* 2003; 63:2292–2299. [PubMed: 12727852]
- Wen T, Zhang Z, Yu Y, Qu H, Koch M, Aumailley M. Integrin alpha3 subunit regulates events linked to epithelial repair, including keratinocyte migration and protein expression. *Wound Repair Regen.* 2010; 18:325–334. [PubMed: 20412552]
- Xia Y, Gill SG, Carter WG. Anchorage mediated by integrin alpha6beta4 to laminin 5 (epiligrin) regulates tyrosine phosphorylation of a membrane associated 80-kD protein. *J Cell Biol.* 1996; 132:727–740. [PubMed: 8647901]
- Yamada KM, Yamada SS, Pastan I. Quantitation of a transformation-sensitive, adhesive cell surface glycoprotein. Decrease of several untransformed permanent cell lines. *J Cell Biol.* 1977; 74:649–654. [PubMed: 328519]
- Zahir N, Lakins JN, Russell A, Ming W, Chatterjee C, Rozenberg GI, et al. Autocrine laminin-5 ligates alpha6beta4 integrin and activates RAC and NFkappaB to mediate anchorage-independent survival of mammary tumors. *J Cell Biol.* 2003; 163:1397–1407. [PubMed: 14691145]

Zhang K, Kramer RH. Laminin 5 deposition promotes keratinocyte motility. *Exp Cell Res.* 1996; 227:309–322. [PubMed: 8831569]

Author Manuscript

Author Manuscript

Author Manuscript

Author Manuscript

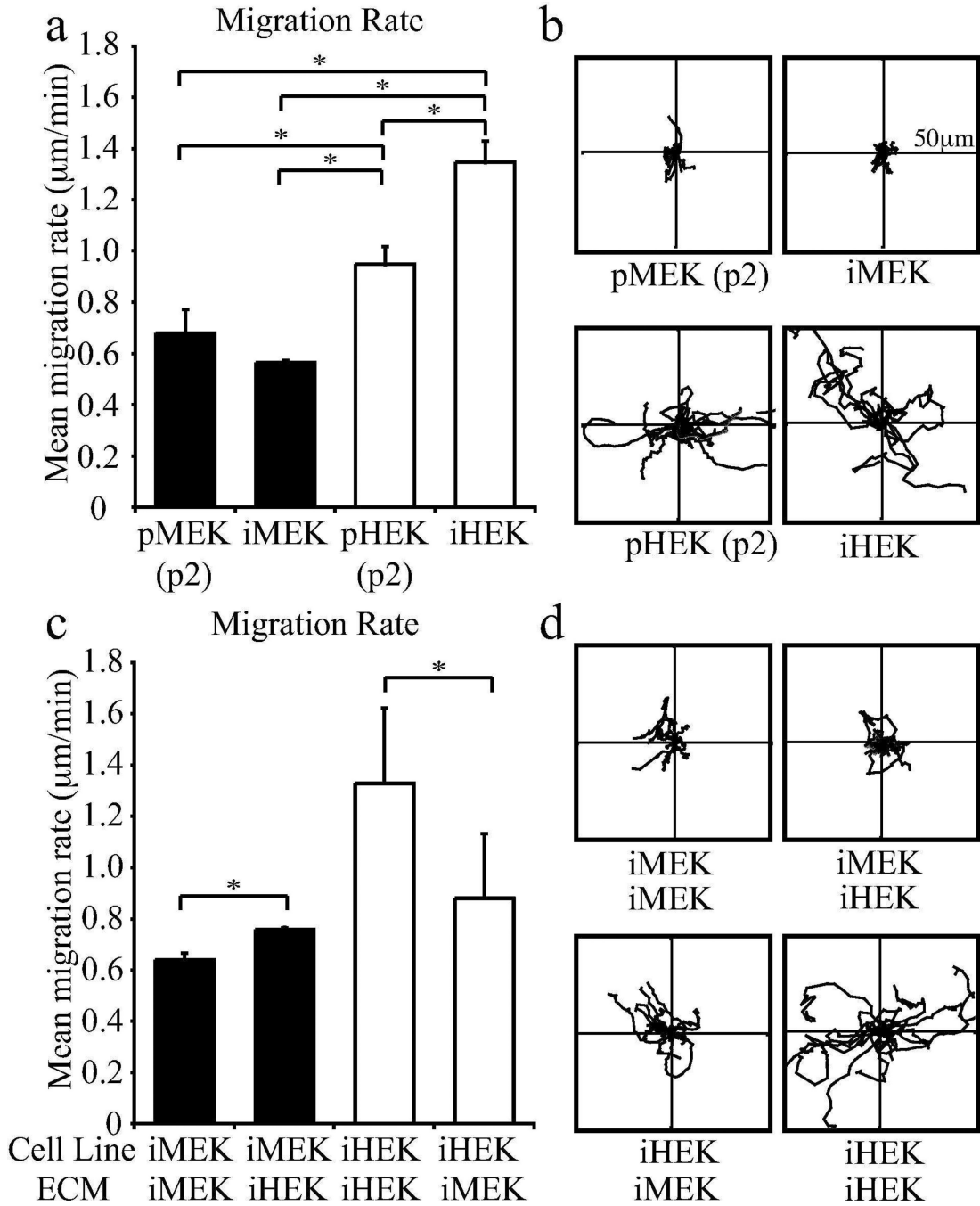


Figure 1.

MEKs migrate with lower velocities than HEKs. In a and b, Passage 2 pMEK, iMEKs, passage 2 pHEKs or iHEKs were plated overnight onto uncoated glass bottomed dishes and images taken every 2 minutes over 1 hour. Individual cells were tracked over the time course of the assay and the mean migration rates plotted. In b, representative vector diagrams depicting the migration tracks of 10 cells are shown. Each line represents the path over which a single cell has migrated relative to its start position. In c and d, iMEKs or iHEKs were plated 80–90% confluence on glass-bottomed dishes. After 24 hours, their

ECMs were prepared. iMEKs or iHEKs were plated onto these ECMs, allowed to adhere for 2 hours then imaged every 2 mins over 1 hour. Individual cells were tracked and their mean migration rates calculated. Representative vector diagrams of 10 cells are shown in d. Graphs in a and b represent mean+SD from a minimum of 3 assays per treatment with >30 cells tracked per assay. * denotes significant differences between grouped populations, $p < 0.01$. Axes of vector diagrams, $50\mu\text{m}$

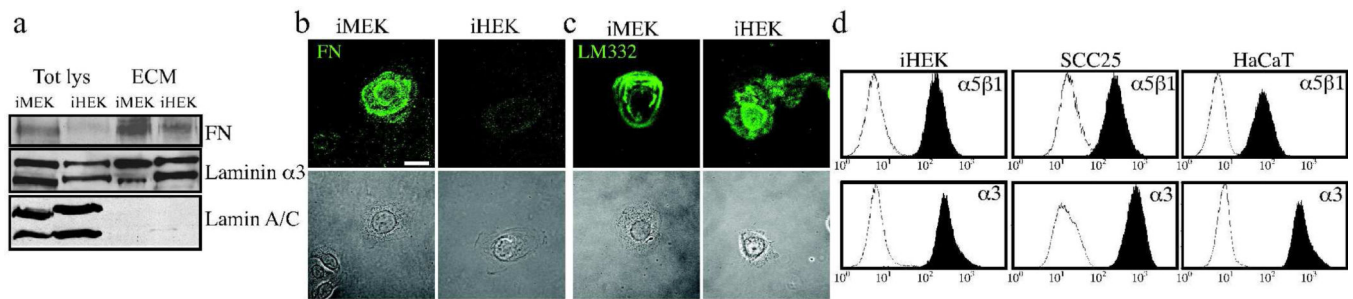


Figure 2.

MEKs deposit more FN than HEKs. In a, iMEKs and iHEKs were plated onto uncoated tissue culture plastic dishes, 24 hours later cell lysates and ECM extracts were prepared for immunoblotting with antibodies against $\alpha 3$ laminin, FN and lamin as indicated. In b and c, iMEKs and iHEKs were plated onto glass coverslips and, 24 hours later, were fixed and then imaged by confocal immunofluorescence microscopy following staining with antibodies against FN(b) or LM332 (c). Phase contrast images are shown in the lower panels. Bar 10 μ m. In c, FACS analyses of cell surface expression of $\alpha 5\beta 1$ and $\alpha 3$ integrin expression was determined for iHEKs, HaCaT, SCC25 as indicated. In each plot the filled trace represents the expression of the indicated antigen while the hollow trace represents non-specific binding when secondary antibody is used alone.

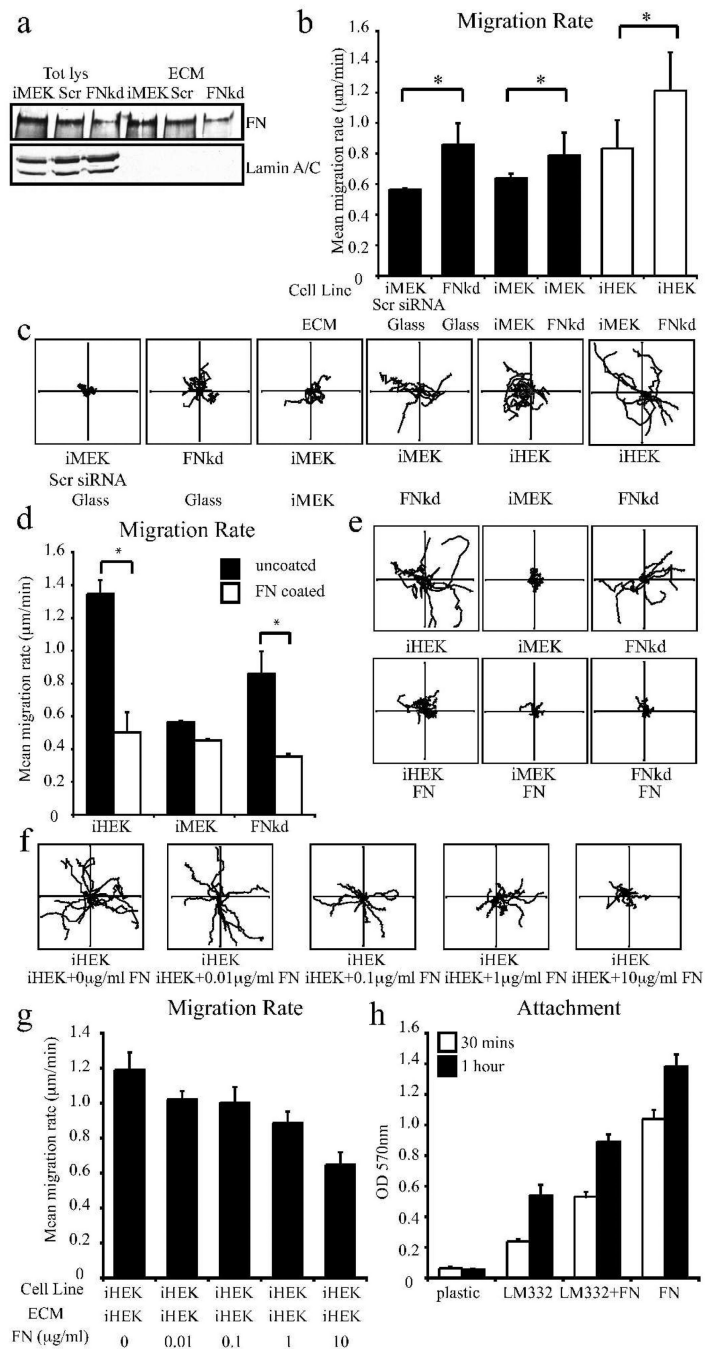


Figure 3. FN knockdown iMEKs display increased migration rates. In a, iMEKs were transiently transfected with either siRNAs targeting FN (FNkd) or scrambled siRNA (Scr). 24 hours later transfected cells were plated onto uncoated tissue culture dishes and allowed to elaborate matrix for 24 hours. Cell lysates and ECM extracts were prepared for immunoblotting with antibodies against FN and lamin as indicated. In b, iMEKs transfected with scrambled siRNA or siRNA against FN were plated onto uncoated glass bottomed dishes overnight and then images taken every 2 mins over 1 hour. The migration of

individual cells was tracked and their mean migration rates determined (b, left 2 columns). In b, columns 3–6, iMEKs or FNsRNA transfected iMEKs were plated on glass-bottomed dishes. 24 hours later their ECM was prepared. Fresh iMEKs or iHEKs were plated for 2 hours onto these ECMs, allowed to adhere for 2 hours then imaged as above. In c, representative vector diagrams of 10 cells viewed over the course of 1h are shown. In d, iHEKs, iMEKs, FNsRNA transfected iMEKs and iMEK α 3- were plated for 2 hours onto FN-coated glass bottomed dishes (coating was at 50 μ g/ml) and their motility rates were determined with representative vector diagrams being shown in e. In f and g, iHEK ECM was prepared then incubated for 1 hour with either PBS alone or with 0.01 to 10 μ g/ml FN in PBS. iHEKs were plated onto the prepared ECM, allowed to attach for 2 hours. In f, representative vector diagrams of 10 cells viewed over the course of the subsequent 1h are shown. with motility rates being displayed in g. In h, attachment of iHEK to the indicated substrates was evaluated at 30 mins and 1 hour after plating. Graphs in b, d and g indicate mean migration rates + SD. Each plot is from a minimum of 3 assays per treatment with >30 cells tracked per assay. * denote significant differences between indicated populations $p < 0.01$. Axes of vector diagrams, 50 μ m. Graph in h represents mean absorbance + SD for assays performed in triplicate.

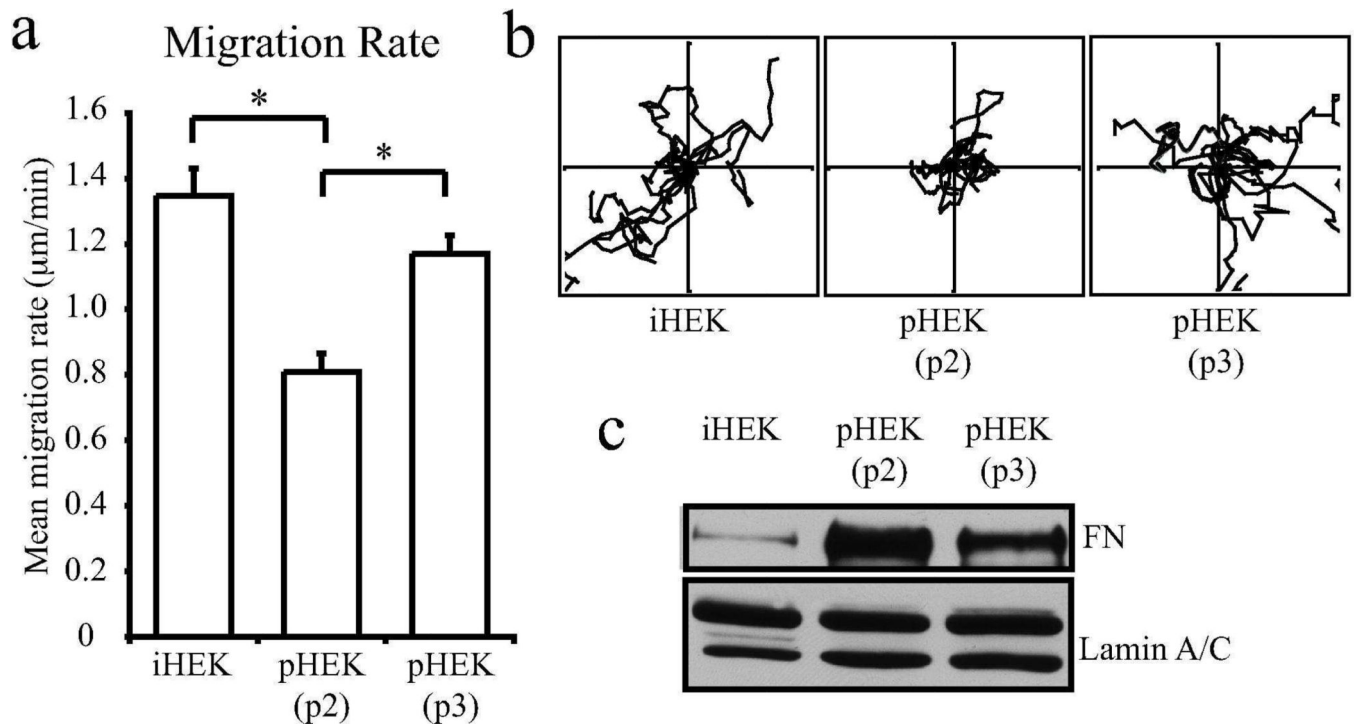


Figure 4.

Migration rates of pHEK increase with increasing passage number. In a, pHEKs were isolated from multiple neonatal foreskins and pooled to make a heterogenous population. At each passage following isolation a subset of cells were plated onto uncoated glass bottomed dishes. The next day images were taken every 2 mins over 1 hour and individual cells tracked. Mean migration rates + SD are plotted from 3 assays >30 cells per assay per passage. * denotes significance $p < 0.01$. In b, representative vector diagrams depicting the migration paths of 10 cells are displayed. Axes, 50µm. In parallel with the motility assays, cell lysates were prepared from the cells at each passage for immunoblotting with antibodies against FN and lamin (c).

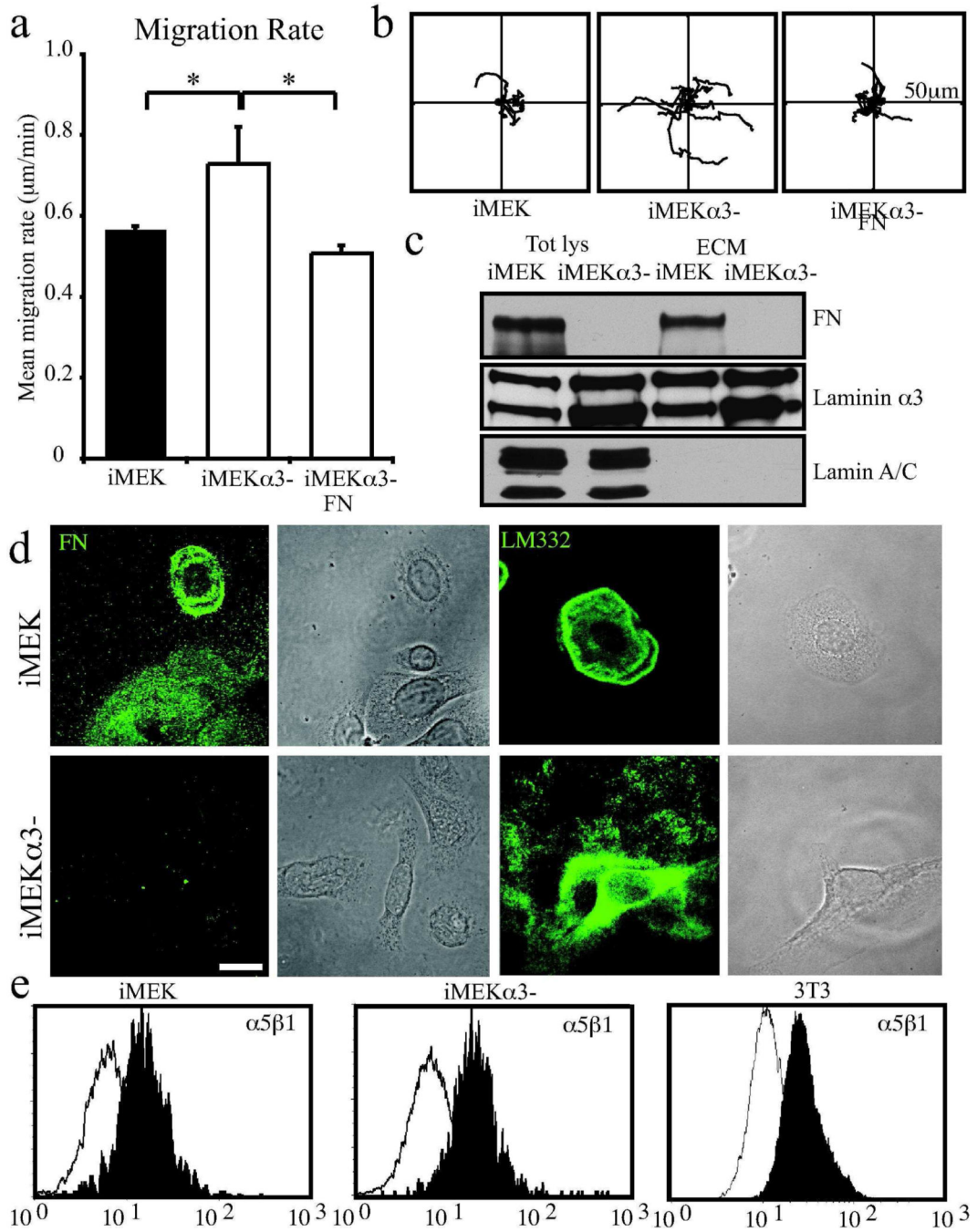


Figure 5.

Integrin α 3 null mouse keratinocytes display enhanced migration rates and express very low levels of FN. In a, iMEK and iMEK α 3- were plated overnight onto uncoated glass bottomed dishes. Cells were imaged every 2 mins for 1 hour and migration paths of individual cells tracked. Graph, depicts mean migration rates + SD from 3 assays per condition >30 cells per assay. * denotes significance $p < 0.01$. In b, representative vector diagrams of 10 MEKs or 10 MEK α 3- cells with each line representing the path of a single cell over the course of the assay relative to its start position, axes 50 μm . In c, total cell lysates and ECMs were

prepared for immunoblotting with antibodies against lamin, FN and $\alpha 3$ laminin, as indicated. In d, iMEK or iMEK $\alpha 3^-$ were plated overnight onto glass coverslips then fixed and imaged by confocal microscopy following staining with antibodies against FN (left panels) or LM332 (right panels), phase contrast images to right of each fluorescent image. Bar 10 μ m. In e, FACS analyses of $\alpha 5\beta 1$ integrin cell surface expression (filled curve) of MEKs, iMEK $\alpha 3^-$ and 3T3 fibroblasts. The latter cells were used as a positive control for the antibody. The hollow curve indicates non-specific secondary antibody reactivity.